The Human-Specific and Smooth Muscle Cell-Enriched LncRNA SMILR Promotes Proliferation by Regulating Mitotic CENPF mRNA and Drives Cell-Cycle Progression Which Can Be Targeted to Limit Vascular Remodeling.

The Human- and Smooth Muscle Cell-Enriched lncRNA SMILR Promotes Proliferation by Regulating Mitotic CENPF mRNA and Drives Cell-Cycle Progression Which Can Be Targeted to Limit Vascular Remodeling

Amira D. Mahmoud[1#], Margaret D. Ballantyne[1#], Vladislav Miscianinov[1], Karine Pinel[1], John Hung[1], Jessica P. Scanlon[1], Jean Iyinikkel[1], Jakub Kaczynski[1], Adriana S. Tavares[1], Angela C. Bradshaw[2], Nicholas L. Mills[1], David E. Newby[1], Andrea Caporali[1], Gwyn W. Gould[3], Sarah J. George[4], Igor Ulitsky[5], Judith C. Sluimer[6,1], Julie Rodor[1], Andrew H. Baker[1,6]*.

[1]Queens Medical Research Institute, BHF Centre for Cardiovascular Sciences, University of Edinburgh, UK, EH16 4TJ; [2]Institute of Cardiovascular and Medical Sciences, BHF Cardiovascular Research Centre, University of Glasgow, UK; [3]Institute of Molecular Cell and Systems Biology, College of Medicine, Veterinary and Life Sciences, University of Glasgow, UK, G12 8QQ; [4]School of Clinical Sciences, University of Bristol, Research Floor Level Seven, Bristol Royal Infirmary, Upper Maudlin St., Bristol BS2 8HW, UK; [5]Department of Biological Regulation, Weizmann Institute of Science, Rehovot, Israel, and; [6]Department of Pathology, Maastricht University Medical Center, Maastricht, the Netherlands

# Equal contributions

***Running title*:** LncRNA SMILR's Mechanism and Therapeutic Potential

Subject Terms:
Basic Science Research
Pathophysiology
Smooth Muscle Cell Proliferation
Translational Studies
Vascular Biology

Address correspondence to:
Dr. Andrew H. Baker
University of Edinburgh
BHF Centre for Cardiovascular Sciences
Queen's Medical Research Institute
47 Little France Crescent
Edinburgh UK
EH16 4TJ
Tel: 0131 24 26728
Andy.Baker@ed.ac.uk

ABSTRACT

***Rationale*:** In response to blood vessel wall injury, aberrant proliferation of vascular smooth muscle cells causes pathologic remodelling. However, the controlling mechanisms are not completely understood.

***Objective*:** We recently showed that the human long non-coding RNA, *SMILR*, promotes vascular smooth muscle cells (vSMCs) proliferation by a hitherto unknown mechanism. Here, we assess the therapeutic potential of *SMILR* inhibition and detail the molecular mechanism of action.

***Methods and Results*:** We used deep RNA-sequencing of human saphenous vein smooth muscle cells stimulated with IL1α and PDGF-BB with SMILR-knockdown (siRNA) or -overexpression (lentivirus), to identify *SMILR* regulated genes. This revealed a SMILR-dependent network essential for cell-cycle progression. In particular, we found using the fluorescent ubiquitination-based cell cycle indicator viral system that SMILR regulates the late mitotic phase of the cell cycle and cytokinesis with *SMILR* knockdown resulting in ~10% increase in binucleated cells. *SMILR*-pulldowns further revealed its potential molecular mechanism, which involves an interaction with the mRNA of the late mitotic protein CENPF and the regulatory Staufen1 RNA-binding protein. *SMILR* and this downstream axis were also found to be activated in the human *ex vivo* vein graft pathological model and in primary human coronary artery smooth muscle cells and atherosclerotic plaques obtained at carotid endarterectomy. Finally, to assess the therapeutic potential of *SMILR*, we used a novel siRNA approach in the *ex vivo* vein graft model (within the 30 min clinical time frame that would occur between harvest and implant) to assess the reduction of proliferation by EdU incorporation. SMILR-knockdown led to a marked decrease in proliferation from ~29% in controls to ~5% with SMILR depletion.

***Conclusion*:** Collectively, we demonstrate that SMILR is a critical mediator of vascular smooth muscle cell proliferation via direct regulation of mitotic progression. Our data further reveals a potential SMILR-targeting intervention to limit atherogenesis and adverse vascular remodelling.

Keywords:
Long non-coding RNA; vascular smooth muscle cells; cell cycle; proliferation; vascular remodelling.

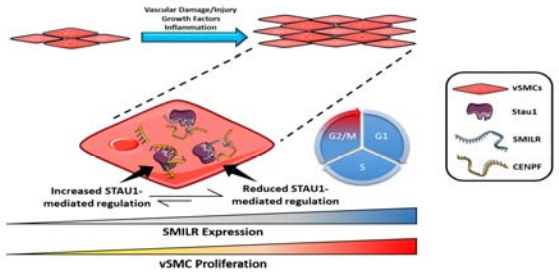

Nonstandard Abbreviations and Acronyms:

vSMCs	Vascular smooth muscle cells
IL1-PDGF	IL1-α and PDGF-ββ-induced
lncRNA	Long non-coding RNA
RNA-seq	RNA-sequencing
PCA	Principal component analysis
HSV	Human saphenous vein
HSVSMCs	Humans saphenous vein derived smooth muscle cells
HCASMCs	Human coronary smooth muscle cells
siRNA	Small interfering RNA
LNT	Lentivirus
GO	Gene ontology
FUCCI	Fluorescence Ubiquitin Cell Cycle Indicator
AurKB	Aurora kinase N
RAP	RNA antisense pulldown
STAU1	Staufen 1 RNA binding protein
FISH	Fluorescence in situ hybridisation

INTRODUCTION

Aberrant proliferation of vascular smooth muscle cells (vSMCs) is a common and functionally important mechanism that impacts on the pathogenesis of many vascular diseases, including intimal thickening associated with remodelling of intra-vascular stents, coronary artery bypass graft failure, atherosclerosis and aortic aneurysm formation. In particular, vSMC proliferation is promoted by the injurious microenvironment, partly through the increased exposure of vSMC to inflammatory cytokines and growth factors such as interleukin-1 (IL-1) and platelet derived growth factor (PDGF), respectively. These often act in synergy to promote a proliferative phenotype with associated activation of critical gene networks, such as metalloproteinases [1-4]. Clinically, targeting vSMC proliferation is exceptionally effective at reducing adverse vascular remodelling following balloon angioplasty and vessel stenting, evidenced by extensive research and development of anti-proliferative drug eluting stent technologies [5, 6]. For iatrogenic vascular injury, pathogenic SMC proliferation causes intimal hyperplasia and luminal narrowing of blood vessels in the setting of vascular stenting or vein graft failure [2, 7]. In more complex settings, such as atherosclerosis, vSMC proliferation is central to the accumulation of large numbers of plaque-derived vSMC that not only contribute to the atherogenic process itself but can also confer plaque stabilisation [8, 9]. Despite context-dependent heterogeneity in vSMC pathobiology, the underlying activation of vSMC proliferation is a central phenotype to the progression of vessel wall dysfunction. It is therefore imperative to further understand the molecular mechanisms that govern vSMC proliferation pathways in order to advance innovative therapies.

Recently, robust evidence has revealed that non-coding RNAs may play a vital role in the regulation of tissue homeostasis, including cardiovascular homeostasis, and hence pathophysiological conditions [10]. Mammalian genomes are pervasively transcribed to produce thousands of long non-coding RNAs (lncRNAs). LncRNAs are widely involved in physiological and pathological processes such as cancer [11], autoimmune diseases [12] and cardiac disease [13]. LncRNA can exert their function via a broad range of activities including, but not limited to, chromatin remodelling, formation of nuclear bodies, and activities as scaffolds and guides [14]. Previous findings have suggested that a substantial proportion of lncRNAs reside within, or are dynamically shuttled to, the cytoplasm in order to regulate mRNA stability, protein translation, microRNA availability and impact upon protein modifications [15]. Such RNA-based regulation generally relies on lncRNA interactions with RNA binding proteins [16]. We previously identified the

lncRNA *SMILR* by RNAseq of human vSMCs following activation by IL-1□ and PDGF-ββ signalling [17]. *SMILR* is an intergenic and poorly conserved lncRNA that consists of only a single 3-exon polyadenylated transcript that is vSMC-enriched, and its knockdown by RNA interference blocked IL-1□ and PDGF-ββ-induced (IL1-PDGF) vSMC proliferation [17]. Thus, we reasoned that identifying the downstream targets and binding partners of *SMILR* would reveal the specific mechanism by which it regulates vSMC proliferation and hence provide a novel therapeutic target for preventing adverse vascular remodelling.

METHODS

The authors declare that all supporting data and materials are available within the article [and its online supplementary files] and available from the corresponding author upon reasonable request. All RNA sequencing data have been made deposited in the Gene Expression Omnibus (GEO) repository, study number GSE120521 for the atherosclerosis RNAseq and GSE117608 for SMILR RNAseq.

Expanded information about materials and methods are available in Online Supplementary Material.

Declaration of Helsinki.
All studies comply with the Declaration of Helsinki, that the locally appointed ethics committee has approved the research protocol and that informed consent has been obtained from the subjects.

Primary human saphenous vein smooth muscle cells (HSVSMC) were isolated via explant technique from consented patients and cultured as previously described [17]. All procedures had local ethical approval (15/ES/0094). HSVSMC from passage 3 to 5 were used for this study and cells were synchronised in DMEM containing 0.2% FBS for 48 h prior to experimentation. Modulation of *SMILR* expression was performed through the utilisation of dsiRNA or SMILR lentivirus with appropriate controls and their effect on the genome was assessed via RNA sequencing and confirmed through subsequent qRT-PCR validation. All qRT-PCR data was analysed via the 2-ΔΔCt method [18]. This method utilises a house keeping gene and ubiquitin C (UBC) was selected as a housekeeping gene due to its stability across all groups and conditions studied. Data is graphed as relative quantification normalized to the UBC housekeeping gene [18].

Assessment of siRNA-SMILR on SMC cell cycle was performed via FUCCI-FACs analysis and confocal imaging for the % of binucleated cells. SiRNA targeting *AURKB* was used as a positive control in these studies as previously described [19, 20].

To evaluate binding partners of *SMILR*, antisense SMILR or GFP probes were designed. For each pulldown experiment either 5 GFP or 5 SMILR probes were utilised to capture bound RNA. Prior to RNA extraction, RNA was spiked with 75ng of total C. elegans RNA and AMA1 used as a reference gene as previously described [21]. qRT-PCR was utilised to assess RNA expression.

To assess if SMILR exhibited any venous/arterial differences in expression or function, human coronary artery smooth muscle cells (HCASMC) were utilise and cultured under the same conditions as HSVSMCs. Stimulation of these cells was performed under basal and IL1/PDGF-BB stimulated conditions as described in Ballantyne et al [17] and assessment of the effect of siRNA-SMILR on HCASMC proliferation (Edu-FACS), binucleation (confocal imaging) and downstream target expression (qRT-PCR) was performed.
To address if SMILR exhibited any protein binding partners, SMILR protein pulldowns were performed utilising streptavidin magnetic beads to capture the biotinylated RNA target and any bound proteins from stimulated smooth muscle cells. Mass spectrometric analysis was utilised to identify proteins for subsequent downstream analysis and validation. Anti-Stau1 pulldowns were utilised as validation with appropriate igG control to confirm SMILR and other RNA target binding by qRT-PCR.

Similar to Ballantyne et. al.[17] patients with symptomatic carotid artery stenosis scheduled to undergo carotid endarterectomy were recruited from neurovascular clinics at the Royal Infirmary of Edinburgh to undergo separate [18F]-fluoride and [18F]- fluorodeoxyglucose ([18F]-FDG) positron emission tomography combined with computed tomography (CT) scans. Regions of stable and unstable plaque were denoted by low and high tracer uptake respectively and appropriately dissected. RNA sequencing was performed to assess transcriptomic differences between plaque sections and SMILR expression assessed via qRT-PCR. In situ hybridisation was utilised to visualise the localisation of SMILR within the plaque regions.

To assess the potential clinical utilisation of siSMILR, segments of human saphenous vein obtained from consented patients undergoing bypass surgery were pinned down with minutien pins on a Sylgard coated dissection dish with the luminal surface facing upward for 0, 7 or 14 days with media refreshed every 2 days. At day 0 and after 7 and 14 days of culture, the vein segments were washed in PBS and snap frozen for subsequent RNA extraction or fixed in 4% PFA for histology. Proliferation of segments was assessed through the utilisation of Click-iT® EdU Alexa Fluor® 488 In Vivo Imaging Kit. Expression levels of SMILR and target RNA were assessed through qRT-PCR analysis. For siRNA transfections HSV segments cut in equal pieces of approximately 1 cm^2 were bathed in PBS containing 25 μM siSMILR and scrambled siRNA control for 30 minutes in 24-well plate. After 30 minutes of incubation, the vein segments were washed with PBS and pinned down as described above. To confirm siRNA transfection, cy3 tagged SMILR was transfected and visualised along with DAPI and αSMA co staining via confocal imaging.

Samples of ≥n=5 were subjected to Shapiro-Wilk test to assess normal distribution followed by student t test or ANOVA. Normal distribution cannot be determined on small samples sizes and samples with n<5 were assumed to be not normally distributed and subjected to Iman and Conover non parametric ranking followed by students t test or ANOVA. Statistical significance $P<0.05$ under all conditions.

RESULTS

Manipulation of SMILR expression identifies a target cell cycle network in HSVSMCs.

SMILR depletion and overexpression was previously shown to decrease and increase, respectively, proliferation induced by stimulation of HSVSMCs with IL1-PDGF [17]. However, no characterisation of the mechanisms of regulation of *SMILR* by IL1-PDGF was described. Accordingly, we sought to identify the potential transcription factor binding sites within the promoter region of *SMILR* (Supplemental Figure IA). Within the 2000bp upstream of *SMILR's* transcription start site, we identified binding sites for transcription factors that are activated by IL1α and/or PDGF-BB including: NF-KB, CEBPβ, ETS1, AP1, NFAT, IRF8, MYB, and AML (Supplemental Figure IB). Of the commercially available transcription factor inhibitors, we analysed the subsequent effects on *SMILR* expression following IL1-PDGF stimulation. This identified that the up-regulation of *SMILR* following IL1-PDGF stimulation may, in part, be due to activation of NF-KB (Supplemental Figure IC and controls in ID). Interestingly, SMILR overexpression does not trigger quiesced HSVSMCs to proliferate in the absence of IL1-PDGF stimulation (Supplemental Figure II). Therefore, to further determine the downstream effects of manipulation of *SMILR* levels on proliferation, RNA-seq was performed on stimulated HSVSMCs exposed to either *SMILR* depletion via siRNA (siSMILR) or overexpression via lentivirus (SMILR LNT) treatment to identify a downstream SMILR-dependent transcriptome (Figure 1A).

Quantification of miR-146a, -221 and -222 by qRT-PCR confirmed activation of the IL1□and PDGF signalling pathways, respectively (Supplemental Figure III) [22, 23]. Alterations in *SMILR* expression levels were validated by qPCR (Figure 1B). Considering a fold change ≥ 1.5 and an adjusted FDR p <

0.05, 523 (334 downregulated and 189 upregulated) and 183 (126 upregulated and 57 down-regulated) transcripts were significantly differentially expressed following knockdown or overexpression, respectively (Figure 1C). As we observe opposing effects on proliferation with *SMILR* knockdown and overexpression, we focused on the transcripts that were dysregulated in opposing levels. This revealed 68 transcripts (Figure 1C and D) indicating that such an approach might be powerful in identifying a distinct *SMILR*-targeted biological interactome. This set of *SMILR*-regulated genes was enriched for cell division-related and nucleosome assembly Gene Ontology (GO) terms (Figure 1E). Interestingly, analysis by STRING [24] identified that 59% (n=40 of 68 genes) of the overlapping genes were associated with a single network involved in progression through the cell cycle, primarily the mitotic phase (Figure 1F). The top 20 genes identified by RNAseq that were differentially regulated genes by *SMILR* (Supplemental Figure IV) were selected for further validation in 3 different patient saphenous vein derived smooth muscle cells by qRT-PCR. We observed consistent and robust opposing regulation of the network following *SMILR* depletion and overexpression in HSVSMCs stimulated with IL1-PDGF (Figure 1G,H). In agreement with the absence of proliferation phenotype after *SMILR* overexpression in non-stimulated quiescent conditions, *SMILR* overexpression in non-stimulated quiescent HSVSMCs did not result in transcription changes of the identified network (Supplemental Figure IIB). Collectively, these data suggest that *SMILR* mechanistically targets the vSMC cell cycle in response to IL1-PDGF stimulation.

Manipulation of SMILR expression effects cell cycle progression in vSMC.

Next, we functionally assessed *SMILR's* ability to directly target cell cycle progression in HSVSMCs. First, we utilised the Fluorescence Ubiquitin Cell Cycle Indicator (FUCCI) viral system as well as flow cytometric analysis to track the cell cycle in synchronised HSVSMCs stimulated with IL1-PDGF for 96 hours with and without *SMILR* knockdown. Following FUCCI viral infection, cells in G0/G1 and S/G2/early M cell cycle phases express mCherry and mAzami-Green (mAG), respectively [25]. Figure 2A represents the colour change predicted in cycling cells, dependent on the relative stage of cell cycle - red (G1), yellow/orange (G1/S) green (G2/early M), or colourless (late M/G0) fluorescence. Aurora kinase B (AurKB), a well-known cell cycle and mitotic mediator, was used as a positive control. Notably, it is also one of *SMILR's* downstream targets in the interactome (Figure 1F). Consistent with previous findings showing IL1-PDGF stimulation only promotes 30% of quiescent cells to proliferate [17], ~60% of the FUCCI-infected HSVSMCs stimulated with IL1-PDGF were found to be colourless under control conditions (Figure 2B and C). Effective knockdown of *AurKB* in the HSVSMCs (4 ± 0.48 fold reduction compared to control, Supplemental Figure V) resulted in a cell cycle defect with a decrease in the G1 phase ($p < 0.05$) and concurrent increase in M/G0 phase ($p < 0.05$; Figure 2B and C). Analysis on FUCCI-infected cells also revealed a clear defect in the G1 phase and increase in the late M/G0 phase of the cell cycle following treatment with siSMILR, thereby phenocopying the effect of *AurKB* knockdown (Figure 2C). A hallmark of such a mitotic phase defect is the inability to correctly segregate daughter from mother cells during cytokinesis, resulting in cellular binucleation [26], which was evident in both FUCCI-infected cells treated with siAurKB and siSMILR (Figure 2D). Accordingly, cells treated with siSMILR and siAURKB were stained with DAPI and phalloidin and assessed for binucleation via fluorescent microscopy (Figure 2E and F). This revealed an increase in the percentage of binucleated cells from 7.2 ± 0.6% and 9.1 ± 0.3% in non-transfected and siControls, respectively, to 17.1 ± 0.4% following *SMILR* depletion ($p < 0.05$), and a similar phenotype was observed in siAurKB-treated cells (20.3 ± 1.6% binucleation) (Figure 2G). Importantly, siRNA treatment had no significant effect on apoptosis with any of the siRNA-based treatments (Figure 2H). Taken together, these data implicate a function for *SMILR* in regulating the late mitotic phase of cell cycle in vSMCs.

SMILR directly targets CENPF in the cell cycle network.

With both overexpression[17] and knockdown (Supplemental Figure IV) approaches affecting *SMILR* expression levels predominantly in the cytoplasmic fraction, we therefore reasoned that *SMILR* could

directly regulate the identified affected genes by binding to the mRNA in the cytoplasm. We used a database of predicted lncRNA-RNA interactions by Terai et al [27] and considered the top100 genes predicted to interact with *SMILR* based on SumEnergy (Supplemental Table I). These genes were analysed in terms of expression level in stimulated vSMC, differential expression in *SMILR* depleted or *SMILR* overexpressed conditions, as well as differential expression upon stimulation with IL1-PDGF (see filtering details in Supplementary methods and summary in Supplemental Table I). This revealed that *CENPF*, a mitotic centromere protein, was the highest ranked mRNA predicted to interact with *SMILR* (minimum and sum energy of -35 and -2631 kcal/mol, respectively, Supplemental Table I). The predicted interacting base pair region of the *SMILR*/*CENPF* mRNA interaction extends across 51 base pairs (39-90) within the sequence of *SMILR* and 58 base pairs (3291-3349) within the coding sequence of *CENPF* transcript (Supplemental Figure VII). We used RNA antisense pulldown (RAP) followed by qRT-PCR to confirm this predicted interaction. Two sets (5 even and 5 odd) of 3′-biotinylated DNA capture oligonucleotides were designed to hybridise specifically to *SMILR* (see Supplementary Methods) [28, 29]. One set of five GFP-specific 3′-biotinylated DNA capture oligonucleotides were also used as a negative control. A schematic overview of the experimental design is provided in Figure 3A. The relative enrichment of *SMILR* and the *CENPF* mRNA present in both the *SMILR*-even and -odd pools were calculated with respect to the GFP pool, which was used as background reference. We observed a 3-fold and 4-fold enrichment of *SMILR* with the even and odd probes, respectively. *CENPF* transcript was also co-enriched by 13-fold and 7-fold in the even and odd *SMILR* pulldowns, respectively, thereby independently validating the predicted interaction between *SMILR* and *CENPF* mRNA. Importantly, MKI67 mRNA another downstream target within the *SMILR*-dependent cell cycle network was assessed in the even and odd *SMILR* pulldowns and found to not to be enriched – suggesting specificity for a *SMILR*: *CENPF* mRNA interaction within the interactome (Figure 3B). Additionally, in agreement with the RNAseq data, *SMILR* depletion and overexpression led to a down- and upregulation of *CENPF* transcript levels, respectively (Figure 3C and D). While having no effect on apoptosis, *CENPF* depletion (Supplemental Figure VIII) resulted in a significant decrease in EdU incorporation (Figure 3E-F). Additionally, similar to previous findings [30, 31], *CENPF* depletion resulted in an increase in the percentage of binucleated cells (12.5 ± 1.2%) comparable to *SMILR* knockdown (13.7 ± 2.2%), which was significantly greater than that observed under control conditions (6.0 ± 2.0%, $p < 0.05$, Figure 3G-H). Importantly, knockdown of *CENPF* also phenotypically mimics the effects of *SMILR* knockdown on key genes within the cell cycle network (Figure 3I). Thus, these data support the concept that *SMILR* positively targets *CENPF* mRNA which is critical for vSMC proliferation.

To further examine the temporal involvement of *SMILR* and *CENPF* transcripts in promoting IL1-PDGF induced proliferation, time course experiments were employed and show that *SMILR* expression is significantly upregulated prior to significant EdU+ incorporation and *CENPF* mRNA expression is detected (Supplemental Figure IX). Taken together, this suggests that *SMILR* is required at the early stages of IL1-PDGF stimulation to promote the induction of proliferation and mitotic progression.

The SMILR:CENPF RNA interaction is regulated by Staufen1.

RNAs, including lncRNAs, have been found to occasionally contain structural motifs that can interact with other RNAs to form functional RNA-RNA hybrids, which can then recruit proteins that regulate their function or stability [32]. Accordingly, to understand whether the function of *SMILR/CENPF* RNA hybrid is dependent on a RNA:protein binding interaction, we performed pulldowns utilising 3'-desthiobiotin-labelled full length *SMILR* and protein lysates from IL1□PDGF stimulated HSVSMCs (Figure 4A). Mass spectrometry identified 14 potential *SMILR*-binding proteins (Figure 4B). The RNA binding protein staufen1 (STAU1), known to be involved in mRNA decay and binds lncRNA and mRNA hybrids [33], was clearly enriched in *SMILR* pulldowns when compared to beads alone or control 3'-desthiobiotin-labelled full length GFP pulldowns (Supplemental Figure X). Moreover, previous reports have suggested that STAU1 is involved in checkpoint decisions in G2 and/or G2/M transitions, which intersects with the cell cycle defects observed with siSMILR [34]. Hence, STAU1 appears to be a prime

candidate partner for SMILR's mechanism of action. Immunoprecipitation of STAU1 from HSVSMC lysates stimulated with IL1−PDGF followed by qRT-PCR revealed enrichment of *SMILR* by 2.8 ± 1 fold ($p < 0.05$) when compared to IgG controls (Figure 4C), validating the mass spectrometry results. Additionally, we found that STAU1 is likely to bind to *SMILR* within the first half of its sequence, which as mentioned above, is the predicted interaction site with CENPF (Supplemental Figure VII and XI). We also identified co-enrichment of *CENPF* in the STAU1 pulldowns by 5.0 ± 2.2 fold ($p < 0.05$; Figure 4C). To explore the involvement of STAU1 in controlling the proliferative phenotype mediated by *SMILR* and *CENPF*, we knocked down STAU1 using dsiRNA, and revealed an increase of *SMILR* and *CENPF* mRNA by 3.3 ± 0.9 fold and 3.0 ± 1.1 fold, respectively (Figure 4D). We accordingly sought to further examine the effect of STAU1 knockdown on the *SMILR* downstream targets. Analysis of the same 20 targets described in Figure 1, which are down- and upregulated following SMILR knockdown and overexpression, revealed that 7 of these genes were significantly upregulated with STAU1 knockdown (Figure 4E). Using RNA FISH, we were also able to examine the co-localisation of *SMILR* and *CENPF* with STAU1 knockdown (Figure 4F). This revealed that, when compared to control conditions, SMILR/CENPF transcript co-localisation is not dependent on STAU1 expression, and that there appears to be increased SMILR/CENPF co-localisation events with STAU1 KD (Figure 4F). Collectively, these data suggests that once *SMILR* expression is upregulated in IL1□PDGF conditions, it is able to bind to *CENPF* mRNA. This may subsequently counteract STAU1-mediated regulation thereby culminating in a proliferative environment and cell cycle progression in vSMCs.

SMILR and the targeted cell cycle network are activated in atherosclerosis and ex vivo vein model of human saphenous vein.

Despite context-dependent heterogeneity in vSMC pathobiology, defects in SMC cell cycle and hence proliferation, are hallmarks of vascular pathologies including atherosclerosis and neointimal hyperplasia associated with vein graft disease [3, 4, 9]. As *SMILR* is poorly-conserved, we are limited to human disease and not animal models to study disease association and causality. To interrogate the *SMILR:CENPF:*STAU1 interaction in human atherosclerosis, we performed an RNAseq on relatively stable and unstable regions dissected from fresh human carotid plaques obtained at carotid endarterectomy in symptomatic patients. Although classified as "stable" these plaques may still contain regions of instability. This is demonstrated by *ex vivo* 18F- sodium fluoride imaging of explanted plaques which was utilised to confirm the appropriate segregation by regions of relatively more unstable versus stable plaque, where increased uptake of the radiotracer [35] was more apparent in "unstable" dissections and less so in the "stable" regions (Figure 5A). Importantly, Principal Component Analysis (PCA) of the RNAseq showed a clear clustering of the distinct regions separately, and not clustering together within each patient sample (Figure 5B). The differential expression analysis confirmed the changes of protein coding genes linked with plaque instability, including those associated with inflammation, matrix remodelling, and calcification (Supplemental Figure XII). *SMILR* expression was upregulated in all unstable plaque samples assessed by qRT-PCR (Figure 5C). Additionally, SMILR was detected using in situ hybridisation with varying intensity across all carotid atherosclerotic plaques from symptomatic patients (Figure D, Supplemental Figure XIII). STAU1 pulldowns in whole carotid plaques also further revealed an interaction with *SMILR* with a 2-fold enrichment compared to IgG controls ($p<0.01$) (Figure 5E). Remarkably, we also observed that 32 of the 40 *SMILR*-dependent cell cycle interactome were also upregulated within the unstable plaques compared to stable, including *CENPF* (Figure 5F and G). Collectively, these data suggest that the *SMILR*/*CENPF*-STAU1 axis is activated in unstable atherosclerosis.

With arterial and venous smooth muscle cells differing significantly, we sought to further investigate the role of *SMILR* in relation to atherosclerosis by validating its mode of action in human coronary artery smooth muscle cells (HCASMCs). Firstly, we confirmed incorporation of EdU in HCASMCs stimulated with IL1-PDGF. This significantly upregulated proliferation, although as previously described ([17], Figure 6A and B), the proliferative capacity of HCASMCs are significantly less than that

observed in the HSVSMCs. Nevertheless, with IL1-PDGF induced proliferation in the HCASMCs, we also identified by qRT-PCR significant increases in *SMILR*, *CENPF*, *MKI67*, *AURKB*, and *CDC20* transcripts (Figure 6C and D). Importantly and similar to that observed in the HSVSMCs, knockdown of *SMILR* and *CENPF* in HCASMCs (Supplemental Figure XIV) resulted in reduction in proliferation (Figure 6E and F). Taken together, this suggests that although arterial and venous smooth muscle cells differ significantly, *SMILR*'s mechanism of action remains consistent.

We also assessed the *SMILR*: *CENPF* axis in the context of vSMC proliferation associated with vein graft disease. Hereto, we used an *ex vivo* human saphenous vein (HSV) model [36,37], which is associated with time-dependent SMC proliferation, migration and formation of neointima over 14 days in culture (Figure 7A) [38]. We first validated this approach by monitoring EdU incorporation at 0, 7, and 14 days and found significant increases (Figure 7B and C). Thus, we hypothesised that *SMILR* expression may be regulated during the culture period. Accordingly, saphenous veins were cultured for 0, 7 or 14 days and the expression of *SMILR*, *CENPF* and the downstream cell cycle associated targets assessed by qRT-PCR. When compared to day 0 control, *SMILR* expression was increased 28 ± 13 ($p < 0.05$) and 53 ± 19 fold ($p < 0.01$), respectively, at day 7 and 14 (Figure 7D). We also identified a time-dependent increase in *CENPF* expression to 8 ± 1 fold ($p < 0.05$) at day 7 and 19 ± 7 fold ($p < 0.05$) at day 14 (Figure 7E). Similar to the qRT-PCR data obtained in Figure 6E, we are able to detect using immunohistochemistry increases in CENPF positive cells in the medial layer from 30% at day 0 to 51% at day 7 (Supplemental Figure XV). Concordantly, expression of other *SMILR* downstream targets within the cell cycle network, namely *AurKB*, *BUB1B*, *MKI67* and *CDC20,* were upregulated at day 7 (22 ± 8, 11 ± 3, 22 ± 8 and 18 ± 7 fold change, respectively) and day 14 (41 ± 14, 34 ± 14, 75 ± 29 and 50 ± 31 fold change, respectively) (Supplemental Figure XVI). Overall, these data suggests that *SMILR* expression and its downstream network has a strong association with pathological remodelling in human *ex vivo* vein grafts.

We then sought to manipulate *SMILR* expression in the *ex vivo* saphenous vein graft to assess the clinical relevance and therapeutic potential. We therefore used a novel siRNA approach within the clinically-relevant time window of an initial 30 minutes (clinical window from harvesting of the saphenous vein to grafting) prior to culture in which to attempt to knockdown *SMILR*. Cy3-tagged siSMILR was first used to visualise the successful infiltration of the siRNA into the vein (Figure 7F). Due to the limitations of the longevity of siRNA chemistry, by day 14 the siSMILR effects were found to be diminished (Supplemental Figure XVII). In veins with siRNA intervention leading to a significant decrease in *SMILR* levels assessed at Day 7 (Figure 7G), we also observed significant decreases in *CENPF* and *MKI67* mRNA expression (Figure 7H and I). Finally, quantified proliferation by EdU incorporation in the cultured vein revealed a strong reduction from 28.7 ± 5.3 % EdU +ve/DAPI +ve nuclei in control conditions to 5.2 ± 2.6 % with *SMILR* knockdown (Figure 7J and K, $p < 0.01$).

DISCUSSION

Aberrant growth of vSMCs is a common and functionally important mechanism, which may ultimately contribute to the etiology of numerous cardiovascular diseases [4]. Although the general mechanism of cell-cycle regulation are well established [39], cell-enriched regulators such as lncRNA are not at all well defined in terms of expression, association and mechanism, which is crucial for the successful development of targeted therapeutics and improved knowledge of how the human transcriptome can impact physiological and pathological pathways. Here, we identify the mechanism and downstream network of the vSMC-enriched human lncRNA, *SMILR*, and demonstrate its therapeutic potential in the *ex vivo* HSV model (Figure 7). This has the potential to not only enhance our understanding of atherogenesis, neointimal hyperplasia and plaque formation, but also provides a clear therapeutic target for future investigation in a broad range of cardiovascular diseases.

The human genome contains a wide range of lncRNAs that are dynamically expressed in a temporal and cell specific manner. These lncRNAs can influence the level and spatial distribution of many proteins and mRNAs in order to control key aspects of cellular function. LncRNAs have previously been shown to modulate cell-cycle, primarily in cancer cell lines [40, 41]. Additionally, lncRNAs, such as smooth muscle and endothelial cell enriched migration/differentiation-associated lncRNA (SENCR) and myocardin-induced smooth muscle lncRNA, inducer of differentiation (MYOSLID), have also been previously shown to be influential in cardiovascular diseases and essential in controlling the phenotypic switching of VSMCs to maintain their contractile phenotype ([42, 43]). More recently, the role of MEG3 in patients with pulmonary arterial hypertension was examined which revealed significantly reduced MEG3 expression levels in patients compared to healthy controls [44]. In vitro siRNA silencing of MEG3 resulted in increased SMC proliferation and migration while mechanistic investigation revealed that MEG3 regulates the p53 pathway in PASMCs [45]. Although several lncRNAs have been identified that control key aspects of SMC and EC function, very little is known about their role in atherosclerosis. A key atherosclerotic lncRNA is ANRIL, which was identified via GWAS studies, in which several SNPs located within this lncRNA were associated with atherosclerosis. It was later identified that ANRIL regulates gene expression epigenetically through recruiting repressive components of the polycomb complexes 1 and 2 to ANRIL-target gene promoters via Alu-repeats [46].

Here, we showed that *SMILR* specifically targets the late mitotic pathway in proliferating HSVSMCs and interacts with *CENPF* mRNA and STAU1. Two recent studies have demonstrated that the lncRNAs, SNHG5 and TINCR, counteract STAU1-mediated decay to promote the stabilisation of specific mRNAs to control tumour cell survival in colorectal cancer and somatic tissue differentiation, respectively [29, 47]. Similar to *TINCR* and its target mRNA *PGLYRP3*, *SMILR's* interaction with *CENPF* mRNA appears to occur independent of STAU1 protein interaction as revealed by RNA-FISH. Although we see up-regulation of both *CENPF* mRNA and *SMILR* with STAU1 knockdown we cannot exclusively conclude whether STAU1's interaction with *SMILR: CENPF* mRNA is regulating *CENPF* at a post-transcriptional and/or post-translational stage. Additionally, STAU1 may not only affect the levels of CENPF at an RNA and/or protein levels but also regulate its sub-cellular localisation since STAU1 has been found to be involved in mRNA transport and localisation to mediate further translation[48].

Whether the *SMILR*/*CENPF* interaction is dependent on base complementarity and/or secondary structure is a key future scientific question as the secondary structure of *SMILR* may be crucial for its localisation, downstream interactions, and hence function [49-51]. Also, other mRNAs might be regulated by *SMILR* and STAU1 and sequencing of associated mRNAs may further provide a comprehensive network of interactions in proliferating vSMCs.

Consistent with our findings, previous studies have indicated that STAU1 primarily binds to protein coding mRNAs of key mediators of cell cycle and that STAU1 expression and function necessarily fluctuates throughout the cell cycle, being highest during the S-phase and rapidly decreasing during mitotic progression [34]. Additionally, STAU1 overexpression affects mitotic entry and impairs proliferation of transformed cells, therefore highlighting STAU1-function must be inhibited in a temporally dependent manner during the cell cycle for proper mitotic progression [34]. With STAU1 being a ubiquitously expressed and a multi-functional protein, lncRNAs may be crucial for providing its cell-specific function and accordingly mediate cell-specific phenotypes. This may also be the case for *CENPF*, which is also ubiquitously expressed and shown to be multi-functional to control mitotic control, transcriptional regulation, and muscle cell differentiation [52]. Intriguingly, increased levels of CENPF have also been previously associated with increased proliferation in malignant conditions [31] and associated with a poor prognosis in human cancers [53, 54]. However, the mechanism by which increased CENPF results in increased proliferation is not entirely understood. One possibility is that the role of CENPF in assembling kinetochore structures required for correct chromosome alignment and separation during mitosis is a rate-limiting step

for mitotic progression. Taken together, our study therefore suggests that *SMILR* may provide such a critical cell-specific regulation of STAU1 and *CENPF* function in human vSMCS to trigger cell cycle progression and proliferation. Further studies are required to dissect mechanistically the consequence of CENPF mRNA regulation by SMILR. Particularly CENPF's mRNA stability, transport, and translation as well as the intersection of this with the mitotic phenotype that we observe when SMILR levels are reduced.

SMILR was previously suggested to function, at least in part, by regulating its neighbouring gene, HAS2[17], although HAS2 is located ≈750kb from SMILR. However, we showed using RNAseq that HAS2 is downregulated with *SMILR* knockdown but was not affected by *SMILR* overexpression, confirming previous findings [17]. We also demonstrated the proliferative effects of *SMILR* occur in the cytoplasmic fraction since the siRNA approach used selectively blocked cytoplasmic *SMILR* expression and would therefore unlikely involve a direct targeting of the HAS2 gene in the nucleus. Here, we focused on the direct regulation by *SMILR* in the cytoplasm and find effects mediated by a distinct proliferative network, but we cannot rule out a downstream effect in the nucleus due to *SMILR* manipulation, or indeed a further proliferative effect mediated selectively in the nucleus by *SMILR* by an independent mechanism. In particular, we noticed the presence of histone mRNAs among the dysregulated genes from the RNAseq data. Although histone mRNAs are not within the list of *SMILR* predicted targets, the observed level change at the RNA level could lead to protein level changes and subsequent transcriptional changes.

The up- or downregulation of the *SMILR*-axis and its consequential effects on vSMC proliferation could influence numerous cardiovascular diseases. This was apparent in the *ex vivo* vein graft model in this study and suggests that this can influence neointimal hyperplasia and hence the long term success of revascularisation of vein graft after coronary artery bypass surgery. Interestingly we found a similar role for SMILR in HCASMCs and may therefore also be involved in atherosclerosis. However targeting of SMILR may not be beneficial due to the potential reduction in stability and formation of a fibrous cap. Further studies are however required to fully understand the influence of the *SMILR*-axis with respect to SMC proliferation in the atherosclerotic environment and hence the susceptibility to plaque rupture and ultimately myocardial infarction and stroke.

Significantly, within a clinically-amenable timeframe, siRNA-based gene therapy targeting *SMILR* is sufficient to markedly reduce proliferation in the *ex vivo* vein model. This excitingly provides a vSMC-specific target, which reduces the possibility of off-target effects in the remainder of the vessel wall, i.e. inhibited re-endothelialisation. This strongly suggests that such an intervention may reduce vein graft failure rates. Although our studies only show successful knockdown with siRNA for a limited time frame, whether this is sufficient to maintain a long term anti-proliferative effect is something that requires further studies. Nonetheless, other routes of *SMILR*-targeting gene therapy may be required for maximum longevity such as LNA-GapmeR antisense oligonucleotides (ASOs) [13]. However, ASOs target both nuclear and cytoplasmic fractions of a cell whereas siSMILR only has a cytoplasmic effect (Supplemental figure 6). Accordingly, the subsequent effects of ASOs knockdown of *SMILR* in the nuclear fraction must be studied to ensure no detrimental effects.

We demonstrate that *SMILR* is a vSMC-enriched lncRNA, essential in the control of cell-cycle through binding of *CENPF* mRNA and STAU1. Our studies provide early but compelling evidence that *SMILR* is an exciting and novel target in the treatment of aberrant growth of vascular smooth muscle cells, with the potential to significantly reduce the rate of vein graft failure.

ACKNOWLEDGEMENTS
We thank Lynne Maquat for her continued advice and to Gregor Aitchison and Yvonne Harcus for technical assistance. We would also like to thank the University of Edinburgh's CALM facility used for flow cytometry and immunofluorescent microscopy.

AUTHOR CONTRIBUTIONS
A.H.B conceived and supervised the study. A.H.B, A.D.M, M.D.B and J.R designed experiments, interpreted data, and wrote the manuscript. A.D.M, M.D.B, V.M, K.P, J.H, and J.P.S. performed experiments. K.P, J.H, J.K and A.S.T sampled and conducted imaging on patient atherosclerotic plaques. J.R. did the RNA-seq analysis. I.U provided pipeline for RNA-seq analysis. G.W.G provided guidance for the cell cycle studies. S.J.G provided guidance on *ex vivo* studies. N.L.M, D.E.N. and J.C.S provided guidance on atherosclerosis and clinical studies. A.C.B and J.C.S provided samples for studies. All the authors discussed the data and edited the manuscript.

DECLARATION OF INTERESTS
The authors declare no competing interests.

SOURCES OF FUNDING
This work is supported by the British Heart Foundation (PG/16/51/32180 and RG/14/3/30706) and the University of Edinburgh's BHF Research Excellence Award (RE/13/3/30183). AHB is supported by the British Heart Foundation Chair of Translational Cardiovascular Sciences (CH/11/2/28733) and European Research Council (EC 338991 VASCMIR).

REFERENCES

1. Patel MI, Ghosh P, Melrose J and Appleberg M. Smooth muscle cell migration and proliferation is enhanced in abdominal aortic aneurysms. *Aust Nz J Surg*. 1996;66:305-308.
2. Marx SO, Totary-Jain H and Marks AR. Vascular smooth muscle cell proliferation in restenosis. *Circulation Cardiovascular interventions*. 2011;4:104-11.
3. Sallam T, Sandhu J and Tontonoz P. Long Noncoding RNA Discovery in Cardiovascular Disease. *Decoding Form to Function*. 2018;122:155-166.
4. Bochaton-Piallat M-L and Bäck M. Novel concepts for the role of smooth muscle cells in vascular disease: towards a new smooth muscle cell classification. *Cardiovascular Research*. 2018;114:477-480.
5. Daemen J and Serruys PW. Drug-eluting stent update 2007: part I. A survey of current and future generation drug-eluting stents: meaningful advances or more of the same? *Circulation*. 2007;116:316-28.
6. Roopmani P, Sethuraman S, Satheesh S and Maheswari Krishnan U. The metamorphosis of vascular stents: passive structures to smart devices. *RSC Advances*. 2016;6:2835-2853.
7. Brancati MF, Burzotta F, Trani C, Leonzi O, Cuccia C and Crea F. Coronary stents and vascular response to implantation: literature review. *Pragmatic and Observational Research*. 2017;8:137-148.
8. Libby P, Ridker PM and Hansson GK. Progress and challenges in translating the biology of atherosclerosis. *Nature*. 2011;473:317-25.
9. Gomez D and Owens GK. Smooth muscle cell phenotypic switching in atherosclerosis. *Cardiovascular Research*. 2012;95:156-164.
10. Uchida S and Dimmeler S. Long Noncoding RNAs in Cardiovascular Diseases. *Circulation Research*. 2015;116:737.
11. Anastasiadou E, Jacob LS and Slack FJ. Non-coding RNA networks in cancer. *Nature reviews Cancer*. 2018;18:5-18.

12. Aune TM, Crooke PS, 3rd, Patrick AE, Tossberg JT, Olsen NJ and Spurlock CF, 3rd. Expression of long non-coding RNAs in autoimmunity and linkage to enhancer function and autoimmune disease risk genetic variants. *Journal of autoimmunity*. 2017;81:99-109.
13. Micheletti R, Plaisance I, Abraham BJ, Sarre A, Ting CC, Alexanian M, Maric D, Maison D, Nemir M, Young RA, Schroen B, Gonzalez A, Ounzain S and Pedrazzini T. The long noncoding RNA Wisper controls cardiac fibrosis and remodeling. *Science translational medicine*. 2017;9.
14. Ulitsky I and Bartel DP. lincRNAs: Genomics, Evolution, and Mechanisms. *Cell*. 2013;154:26-46.
15. Rashid F, Shah A and Shan G. Long Non-coding RNAs in the Cytoplasm. *Genomics, Proteomics & Bioinformatics*. 2016;14:73-80.
16. Barra J and Leucci E. Probing Long Non-coding RNA-Protein Interactions. *Frontiers in molecular biosciences*. 2017;4:45.
17. Ballantyne MD, Pinel K, Dakin R, Vesey AT, Diver L, Mackenzie R, Garcia R, Welsh P, Sattar N, Hamilton G, Joshi N, Dweck MR, Miano JM, McBride MW, Newby DE, McDonald RA and Baker AH. Smooth Muscle Enriched Long Noncoding RNA (SMILR) Regulates Cell Proliferation. *Circulation*. 2016;133:2050-65.
18. Livak KJ and Schmittgen TD. Analysis of Relative Gene Expression Data Using Real-Time Quantitative PCR and the 2−ΔΔCT Method. *Methods*. 2001;25:402-408.
19. Goto H, Yasui Y, Kawajiri A, Nigg EA, Terada Y, Tatsuka M, Nagata K and Inagaki M. Aurora-B regulates the cleavage furrow-specific vimentin phosphorylation in the cytokinetic process. *J Biol Chem*. 2003;278:8526-30.
20. Goldenson B and Crispino JD. The aurora kinases in cell cycle and leukemia. *Oncogene*. 2015;34:537-45.
21. Zhang Y, Chen D, Smith MA, Zhang B and Pan X. Selection of reliable reference genes in Caenorhabditis elegans for analysis of nanotoxicity. *PLoS One*. 2012;7:e31849.
22. Gu S-X, Li X, Hamilton JL, Chee A, Kc R, Chen D, An HS, Kim J-S, Oh C-d, Ma Y-Z, van Wijnen AJ and Im H-J. MicroRNA-146a reduces IL-1 dependent inflammatory responses in the intervertebral disc. *Gene*. 2015;555:80-87.
23. Taganov KD, Boldin MP, Chang K-J and Baltimore D. NF-κB-dependent induction of microRNA miR-146, an inhibitor targeted to signaling proteins of innate immune responses. *Proceedings of the National Academy of Sciences of the United States of America*. 2006;103:12481-12486.
24. Szklarczyk D, Morris JH, Cook H, Kuhn M, Wyder S, Simonovic M, Santos A, Doncheva NT, Roth A, Bork P, Jensen LJ and von Mering C. The STRING database in 2017: quality-controlled protein-protein association networks, made broadly accessible. *Nucleic Acids Res*. 2017;45:D362-D368.
25. Zielke N and Edgar BA. FUCCI sensors: powerful new tools for analysis of cell proliferation. *Wiley interdisciplinary reviews Developmental biology*. 2015;4:469-87.
26. Terada Y. Role of chromosomal passenger complex in chromosome segregation and cytokinesis. *Cell structure and function*. 2001;26:653-7.
27. Terai G, Iwakiri J, Kameda T, Hamada M and Asai K. Comprehensive prediction of lncRNA–RNA interactions in human transcriptome. *BMC Genomics*. 2016;17:12.
28. Engreitz JM, Pandya-Jones A, McDonel P, Shishkin A, Sirokman K, Surka C, Kadri S, Xing J, Goren A, Lander ES, Plath K and Guttman M. The Xist lncRNA Exploits Three-Dimensional Genome Architecture to Spread Across the X Chromosome. *Science*. 2013;341.
29. Kretz M, Siprashvili Z, Chu C, Webster DE, Zehnder A, Qu K, Lee CS, Flockhart RJ, Groff AF, Chow J, Johnston D, Kim GE, Spitale RC, Flynn RA, Zheng GXY, Aiyer S, Raj A, Rinn JL, Chang HY and Khavari PA. Control of somatic tissue differentiation by the long non-coding RNA TINCR. *Nature*. 2013;493:231-235.
30. Bomont P, Maddox P, Shah JV, Desai AB and Cleveland DW. Unstable microtubule capture at kinetochores depleted of the centromere-associated protein CENP-F. *The EMBO journal*. 2005;24:3927-39.

31. Holt SV, Vergnolle MAS, Hussein D, Wozniak MJ, Allan VJ and Taylor SS. Silencing Cenp-F weakens centromeric cohesion, prevents chromosome alignment and activates the spindle checkpoint. *Journal of Cell Science*. 2005;118:4889.
32. Guil S and Esteller M. RNA-RNA interactions in gene regulation: the coding and noncoding players. *Trends in Biochemical Sciences*. 2015;40:248-256.
33. Gong C and Maquat LE. lncRNAs transactivate STAU1-mediated mRNA decay by duplexing with 3' UTRs via Alu elements. *Nature*. 2011;470:284-8.
34. Boulay K, Ghram M, Viranaicken W, Trepanier V, Mollet S, Frechina C and DesGroseillers L. Cell cycle-dependent regulation of the RNA-binding protein Staufen1. *Nucleic Acids Res*. 2014;42:7867-83.
35. Joshi NV, Vesey AT, Williams MC, Shah ASV, Calvert PA, Craighead FHM, Yeoh SE, Wallace W, Salter D, Fletcher AM, van Beek EJR, Flapan AD, Uren NG, Behan MWH, Cruden NLM, Mills NL, Fox KAA, Rudd JHF, Dweck MR and Newby DE. 18F-fluoride positron emission tomography for identification of ruptured and high-risk coronary atherosclerotic plaques: a prospective clinical trial. *The Lancet*. 2014;383:705-713.
36. Soyombo AA, Angelini GD, Bryan AJ, Jasani B and Newby AC. Intimal proliferation in an organ culture of human saphenous vein. *The American journal of pathology*. 1990;137:1401-10.
37. Angelini GD, Soyombo AA and Newby AC. Winner of the ESVS prize 1990. Smooth muscle cell proliferation in response to injury in an organ culture of human saphenous vein. *European journal of vascular surgery*. 1991;5:5-12.
38. George SJ, Johnson JL, Angelini GD, Newby AC and Baker AH. Adenovirus-mediated gene transfer of the human TIMP-1 gene inhibits smooth muscle cell migration and neointimal formation in human saphenous vein. *Human gene therapy*. 1998;9:867-77.
39. Musacchio A and Salmon ED. The spindle-assembly checkpoint in space and time. *Nature Reviews Molecular Cell Biology*. 2007;8:379.
40. Nötzold L, Frank L, Gandhi M, Polycarpou-Schwarz M, Groß M, Gunkel M, Beil N, Erfle H, Harder N, Rohr K, Trendel J, Krijgsveld J, Longerich T, Schirmacher P, Boutros M, Erhardt S and Diederichs S. The long non-coding RNA LINC00152 is essential for cell cycle progression through mitosis in HeLa cells. *Scientific Reports*. 2017;7:2265.
41. Hu WL, Jin L, Xu A, Wang YF, Thorne RF, Zhang XD and Wu M. GUARDIN is a p53-responsive long non-coding RNA that is essential for genomic stability. *Nature Cell Biology*. 2018;20:492-502.
42. Lyu Q, Xu S, Lyu Y, Choi M, Christie CK, Slivano OJ, Rahman A, Jin ZG, Long X, Xu Y and Miano JM. SENCR stabilizes vascular endothelial cell adherens junctions through interaction with CKAP4. *Proceedings of the National Academy of Sciences of the United States of America*. 2019;116:546-555.
43. Zhao J, Zhang W, Lin M, Wu W, Jiang P, Tou E, Xue M, Richards A, Jourd'heuil D, Asif A, Zheng D, Singer HA, Miano JM and Long X. MYOSLID Is a Novel Serum Response Factor-Dependent Long Noncoding RNA That Amplifies the Vascular Smooth Muscle Differentiation Program. *Arteriosclerosis, thrombosis, and vascular biology*. 2016;36:2088-99.
44. Sun Z, Nie X, Sun S, Dong S, Yuan C, Li Y, Xiao B, Jie D and Liu Y. Long Non-Coding RNA MEG3 Downregulation Triggers Human Pulmonary Artery Smooth Muscle Cell Proliferation and Migration via the p53 Signaling Pathway. *Cell Physiol Biochem*. 2017;42:2569-2581.
45. Jae N, Heumuller AW, Fouani Y and Dimmeler S. Long non-coding RNAs in vascular biology and disease. *Vascul Pharmacol*. 2019;114:13-22.
46. Holdt LM, Hoffmann S, Sass K, Langenberger D, Scholz M, Krohn K, Finstermeier K, Stahringer A, Wilfert W, Beutner F, Gielen S, Schuler G, Gabel G, Bergert H, Bechmann I, Stadler PF, Thiery J and Teupser D. Alu elements in ANRIL non-coding RNA at chromosome 9p21 modulate atherogenic cell functions through trans-regulation of gene networks. *PLoS Genet*. 2013;9:e1003588.
47. Damas ND, Marcatti M, Côme C, Christensen LL, Nielsen MM, Baumgartner R, Gylling HM, Maglieri G, Rundsten CF, Seemann SE, Rapin N, Thézenas S, Vang S, Ørntoft T, Andersen CL, Pedersen JS and Lund AH. SNHG5 promotes colorectal cancer cell survival by counteracting STAU1-mediated mRNA destabilization. *Nature Communications*. 2016;7:13875.

48. Park E and Maquat LE. Staufen-mediated mRNA decay. *Wiley Interdiscip Rev RNA*. 2013;4:423-35.
49. Brown JA, Valenstein ML, Yario TA, Tycowski KT and Steitz JA. Formation of triple-helical structures by the 3'-end sequences of MALAT1 and MENbeta noncoding RNAs. *Proc Natl Acad Sci U S A*. 2012;109:19202-7.
50. Novikova IV, Hennelly SP and Sanbonmatsu KY. Sizing up long non-coding RNAs: do lncRNAs have secondary and tertiary structure? *Bioarchitecture*. 2012;2:189-99.
51. Somarowthu S, Legiewicz M, Chillon I, Marcia M, Liu F and Pyle AM. HOTAIR forms an intricate and modular secondary structure. *Molecular cell*. 2015;58:353-61.
52. Ma L, Zhao X and Zhu X. Mitosin/CENP-F in mitosis, transcriptional control, and differentiation. *Journal of Biomedical Science*. 2006;13:205-213.
53. Zhuo YJ, Xi M, Wan YP, Hua W, Liu YL, Wan S, Zhou YL, Luo HW, Wu SL, Zhong WD and Wu CL. Enhanced expression of centromere protein F predicts clinical progression and prognosis in patients with prostate cancer. *International journal of molecular medicine*. 2015;35:966-72.
54. O'Brien SL, Fagan A, Fox EJP, Millikan RC, Culhane AC, Brennan DJ, McCann AH, Hegarty S, Moyna S, Duffy MJ, Higgins DG, Jirström K, Landberg G and Gallagher WM. CENP-F expression is associated with poor prognosis and chromosomal instability in patients with primary breast cancer. *International journal of cancer*. 2007;120:1434-1443.

FIGURE LEGENDS

Figure 1. Transcriptomics identifies a cell cycle-associated network targeted by SMILR in proliferative vSMCs.
(A) Schematic of experimental design for *SMILR* knockdown and overexpression using dsiRNA and lentivirus (LNT), respectively. MOI = multiplicity of infection. (B) Validation of *SMILR* knockdown and overexpression via qRT-PCR of 3 technical replicates used for RNAseq from one patient sample. (C) Venn diagrams illustrating the number of genes dysregulated by *SMILR* knockdown and overexpression. (D) Heatmap of all overlapping 68 significant changes observed upon *SMILR* depletion and overexpression. Fold change calculated compared to the average FPKM in the control (CONT) samples. (E) Gene Ontology (GO) terms for the *SMILR*-regulated gene cohort. (F) Protein network of 40 proliferative and cell-cycle associated genes found to be dysregulated with *SMILR* depletion and overexpression. (G,H) Further validation by qRT-PCR of the top 20 identified dysregulated proliferative and cell-cycle associated genes with siRNA Control (siCtrl) versus siSMILR and control LNT (Null LNT) versus SMILR LNT. * = $p < 0.05$, by Iman and Conover non parametric ranked paired student's t-test of deltaCT values between gene of interest and the housekeeper gene UBC, n = 3 biological replicates.

Figure 2. *SMILR* manipulation regulates the cell cycle of vSMC.
(A) Schematic of FUCCI viral analysis. (B) Flow cytometric analysis tracking cell cycle changes indicated by colour changes of the FUCCI viruses. (C) Bar chart representing average changes in the % of cells in each stage of the cell cycle. Repeated measures ANOVA for * $p<0.05$, Iman and Conover ranked non parametric analysis followed by one way ANOVA, n = 3 biological replicates. (D) Fluorescent Microscopy of HSVSMCs infected with the FUCCI viral system. Scale bars at 50 μm. Red arrows indicate binucleated cells. (E) Schematic of characterisation method of binucleated cells. (F) Fluorescent images of HSVSMCs stained with DAPI and phalloidin. Scale bars at 50 μm. Red arrows indicate binucleated cells. (G) Bar chart representing the % of total cells that were binucleated. * = $p < 0.05$, Iman and Conover ranked non parametric analysis followed by one way ANOVA vs IL1α/PDGF-ββ treatment alone (I+P); + = $p < 0.05$ vs siControls, n = 3 biological replicates. (H) Bar chart representing caspase-3 activity in HSVSMCs cultured with siRNA or hydrogen peroxide as a positive control. Caspase activity measured by OD405. n = 3 biological replicates, vs I+P treatment. ns = not significant.

Figure 3. RNA: RNA analysis reveal a SMILR: CENPF interaction.
(A) Schematic of DNA antisense biotinylated probes site for *SMILR* and *GFP* and the experimental design of RNA: RNA pulldowns. (B) Bar charts representing relative enrichments of *SMILR*, *CENPF*, and *MKI67* in SMILR even and odd pulldowns versus the GFP control pulldown. Each even and odd SMILR probe pulldown was performed once across two independent biological replicates. Effects of **(C)** *SMILR* knockdown and **(D)** *SMILR* overexpression on *CENPF* mRNA. ** = $p < 0.05$ Iman and Conover non parametric ranked analysis followed by students t-test, n = 3 biological replicates. **(E)** Representative FACs histogram plots depicting EdU uptake in siCtrl and siCENPF treated HSVSMCs. Gate represents EdU+ cells. **(F)** Bar chart showing mean changes of EdU incorporation in siCtrl and siCENPF treated HSVSMCs. Iman and Conover ranked non parametric analysis followed by t-test, n=3 biological replicates. * = $p < 0.05$. (G) Fluorescent images of HSVSMCs stained with DAPI and phalloidin. Scale bar represents 50 μm. Red arrows indicate binucleated cells. (H) Bar chart representing the % of total cells that were binucleated. Iman and Conover ranked non parametric analysis followed by students t-test * = $p < 0.05$vs siCtrl, n = 3 biological replicates. (I) The effects of *CENPF* knockdown on mitotic associated genes compared to effects observed with knockdown of *SMILR*, * = $p < 0.05$, by Iman and Conover ranked non parametric analysis followed by paired t-test, n = 4 biological replicates.

Figure 4. STAU1 degrades the *SMILR*: *CENPF* interaction to mediate vSMC proliferation.
(A) Schematic showing methodology of biotinylated *SMILR*-pulldowns. (B) Mass spectrometry identified 14-enriched *SMILR*-binding proteins. Staufen1 (STAU1) was specifically enriched in the *SMILR* pulldown

with 11-unique peptides detected. (C) Anti-STAU1 pulldowns confirming interaction with *SMILR* and *CENPF*; * = p < 0.05, by Iman and Conover ranked non parametric analysis followed by t-test, n = 3 pulldowns from 3 independent patient samples. (D) Relative quantification of STAU1, *SMILR*, and *CENPF* expression with SiSTAU1 at 10nM. * = p < 0.05, by Iman and Conover ranked non parametric analysis followed by t-test, n = 3 biological replicates. (E) The effects of STAU1 knockdown on the top 20 downregulated cell-cycle associated genes regulated by *SMILR*, * = p< 0.05, by Iman and Conover ranked non parametric analysis followed by t-test, n = 3 biological replicates. (F) RNA fluorescence in situ hybridization (FISH) for *SMILR* (red) and *CENPF* (green) in stimulated vSMCs under control, siSMILR, siCENPF, and siSTAU1 conditions. Scale bar represents 20 μm. Yellow arrows show some co-localisation events.

Figure 5. *SMILR* and the targeted cell cycle network are activated in atherosclerosis
(A) *Ex vivo* 18F imaging of unstable versus stable plaques. (B) Principal Component Analysis (PCA) of the RNAseq of the stable and unstable samples. (C) Relative FPKMs of protein coding genes linked with plaque instability, including those associated with inflammation and calcification. (D) Representative images of in situ detection of *SMILR* in plaques obtained from the carotid artery derived from symptomatic patients at carotid endarterectomy (n = 5 biological replicates per plaque type, replicates in Supplemental Figure 12). *SMILR* is visualised using NBT/BCIP (purple) at varying intensities across plaques exhibiting either intraplaque haemorrhage or thick fibrous cap. Nuclei are stained with fast red. L, indicates arterial lumen; NC, lipid core; scale bar represents 200 μm (E) *SMILR* enrichment in STAU1 pulldowns in whole carotid plaques, n = 6, ** = p < 0.01, by paired student t-test with paired experiments matched by colour. Protein network (F) and heatmap (G) of the 34 proliferative and cell-cycle associated genes found to be dysregulated with *SMILR* manipulation and unregulated in unstable plaques.

Figure 6. Role of SMILR in human coronary artery smooth muscle cells.
(A) Representative FACs histogram plots depicting EdU uptake in 0.2% and I+P treated HCASMCs. Gate represents EdU+ cells. (B) Bar chart showing mean changes of EdU incorporation in 0.2% and I+P conditions. Iman and Conover ranked non parametric analysis followed by t-test, n=3 biological replicates. * = p < 0.05. Bar charts showing relative expression of (C) SMILR and (D) CENPF, MKI67, AURKB, and CDC20 by qRT-PCR in 0.2% and I+P stimulated HCASMCs. Iman and Conover ranked non parametric analysis followed by t-test, n=3 biological replicates. ** = p < 0.05. (E) Representative FACs histogram plots depicting EdU uptake in siCtrl, siSMILR, and siCENPF treated HCASMCs. Gate represents EdU+ cells. (F) Bar chart showing mean changes of EdU incorporation in siCtrl, siSMILR, and siCENPF treated cells. Iman and Conover ranked non parametric analysis followed by t-test, n=3 biological replicates, * = p < 0.05.

Figure 7. SMILR modulates the proliferation of the *ex vivo* human saphenous vein organ culture. (A) Graphical representation of *ex vivo* HSV proliferation model. (B) Quantification of EdU +ve nuclei in the media of HSV in culture expressed as % of EdU +ve/DAPI +ve nuclei. # = p < 0.05, * = p < 0.0,. * versus Day 0, # versus Day 7 using Iman and Conover ranked non parametric analysis followed by one-way ANOVA (n=3 biological replicates per time point). (C) Representative images of HSV in culture stained for EdU (green) and with DAPI (blue) at day 0, 7, and 14 (n = 3 biological replicates per time point). SMILR (D) and CENPF (E) expression determined by qRT-PCR analysis at day 0, 7 and 14. * P<0.05 and *** P<0.001 vs day 0 analysed by one way ANOVA (n=7). (F) Left: Graphical representation of the model of HSV siSMILR intervention; Right: Representative image of Cy3-labeled *SMILR* siRNA localization in HSV at 3 days post-siSMILR intervention; the section is co-stained with DAPI (blue) and for α-smooth muscle actin (αSMA, green) at 60x magnification. Relative quantification of (G) *SMILR*, (H) CENPF, and (I) MKI67 expression in HSV after siSMILR intervention at day 7 normalized to UBC. * = p < 0.05, ** = p < 0.01 by paired two-tailed Student's t-test, n = 5 biological replicates. (J) Representative images of HSV post-siSMILR intervention stained for EdU (green) and with DAPI (blue). (K) Mean ± SEM of EdU +ve nuclei in the media of HSV after siSMILR intervention expressed as % of EdU +ve/DAPI +ve nuclei. (n

= 3 biological replicates). Values are * = $p < 0.05$; vs siCtrl using Iman and Conover ranked non parametric analysis followed by student's t-test.

NOVELTY AND SIGNIFICANCE

What Is Known?

- Like other non-coding RNA, long non-coding RNA (lncRNA) can regulate key aspects of smooth muscle cell function.
- LncRNA *SMILR* regulates SMC proliferation via an unknown mechanism.

What New Information Does This Article Contribute?

- LncRNA *SMILR* regulates a network of cell cycle-associated mRNAs in vascular smooth muscle cells.
- LncRNA *SMILR* binds directly to the mitotic cell regulator centromere protein F (CENPF) mRNA.
- Inhibition of SMILR by RNA interference blocks vascular smooth muscle cell proliferation in intact saphenous vein.

VSMC proliferation has been recognised as central to the pathology of many major forms of vascular disease including intimal hyperplasia associated with vein graft failure. Previously, RNA-sequencing identified *SMILR* as a novel intergenic lncRNA activated by vSMC proliferation. Understanding the molecular mechanisms governing the mode of action of *SMILR* is an important next step. Specific modulation of *SMILR* levels revealed its role in regulating a mitotic mRNA network and more specifically a central role for binding to the cell cycle associated CENPF mRNA. Specific knockdown of *SMILR* resulted in the accumulation of binucleated cells and reduced proliferation and was phenotypically copied by silencing of CENPF. Further, we show that *SMILR* binds the RNA-binding protein Stau1 which may aid in the regulation of cell cycle. Finally, *SMILR* inhibition in whole vein segments resulted in the reduction of SMC proliferation through modulation of the key cell cycle network. Our findings provide compelling evidence that *SMILR* is a novel target in the treatment of aberrant growth of vascular smooth muscle cells.

FIGURE 1

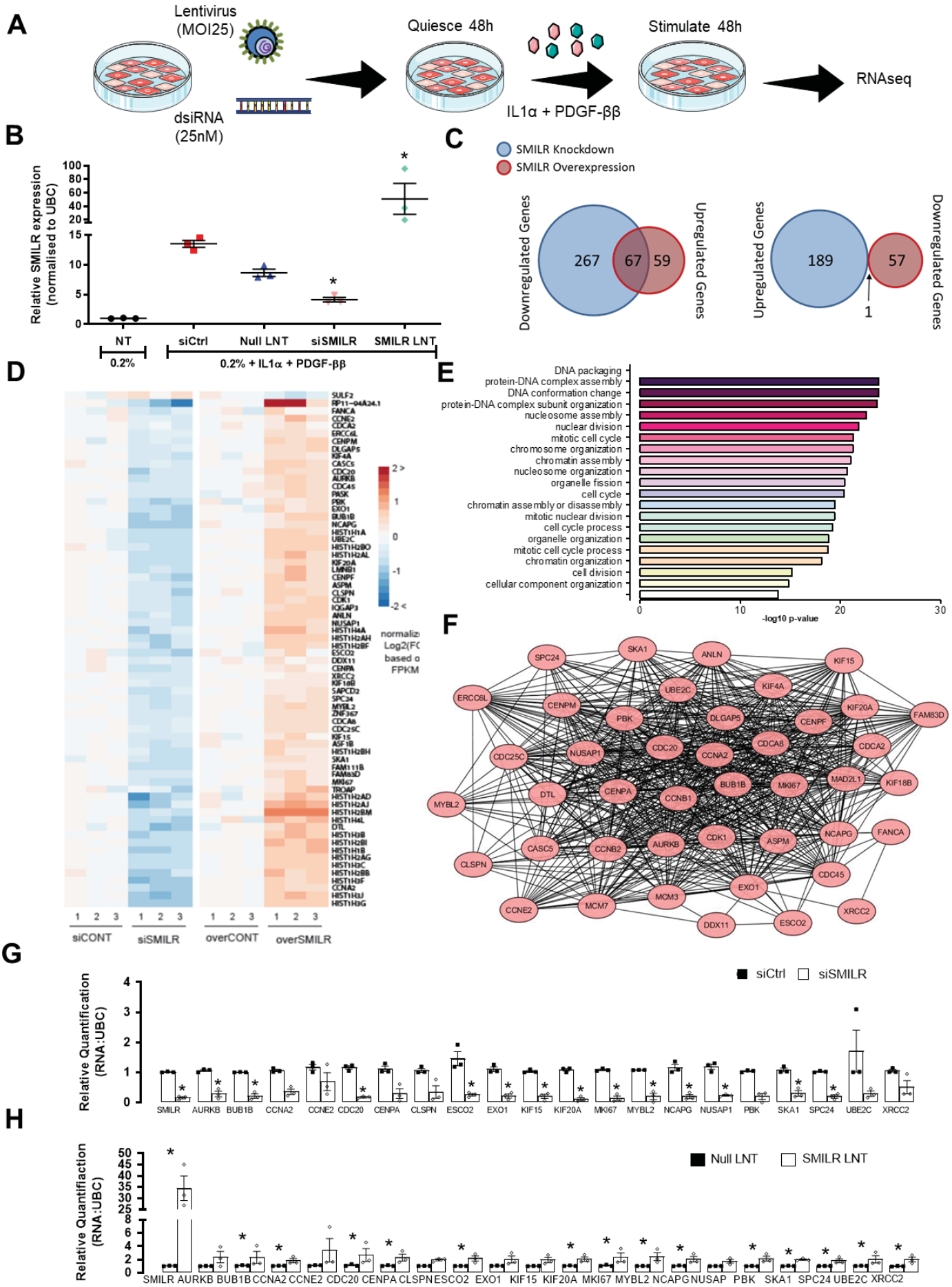

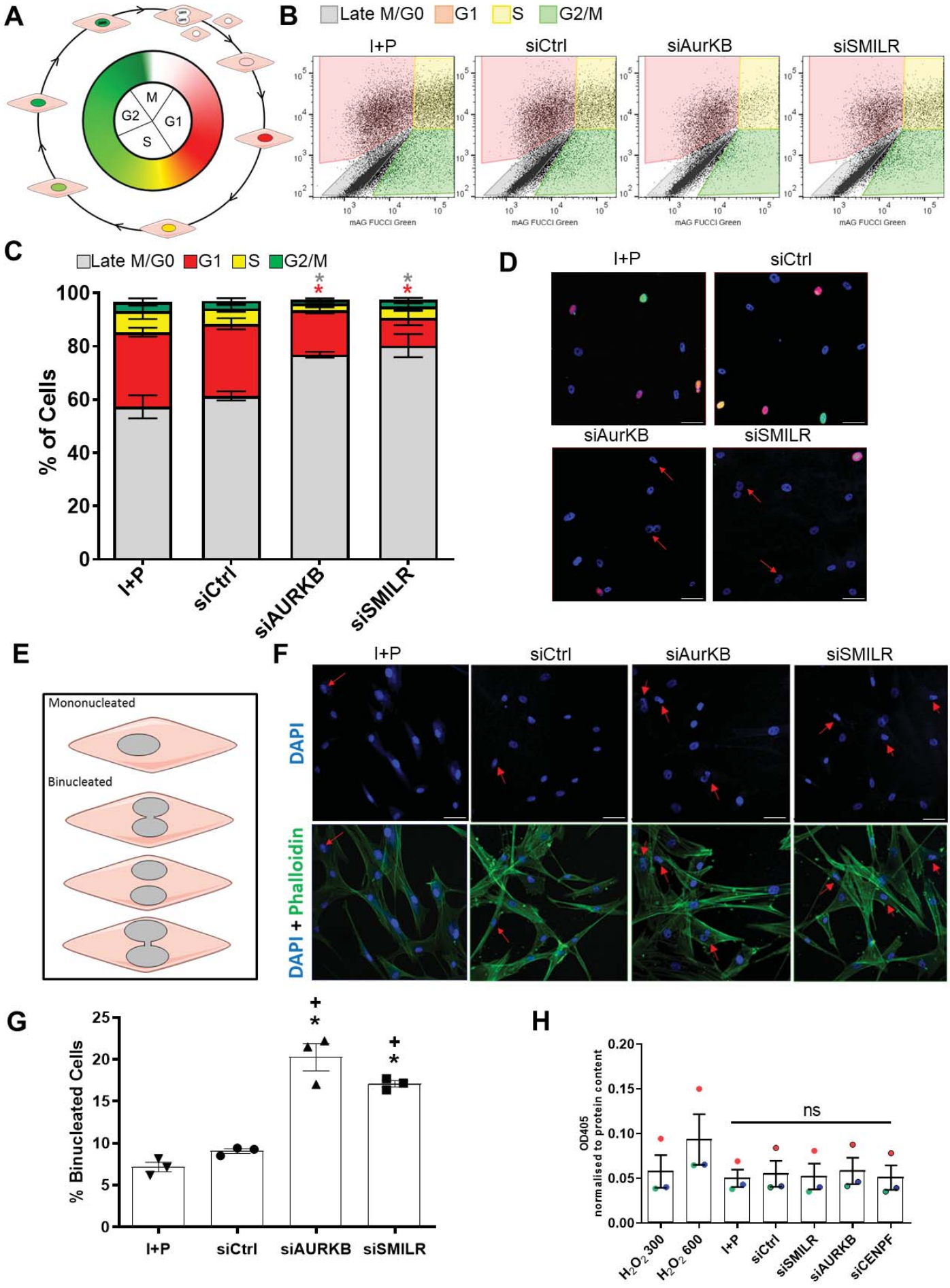

FIGURE 3

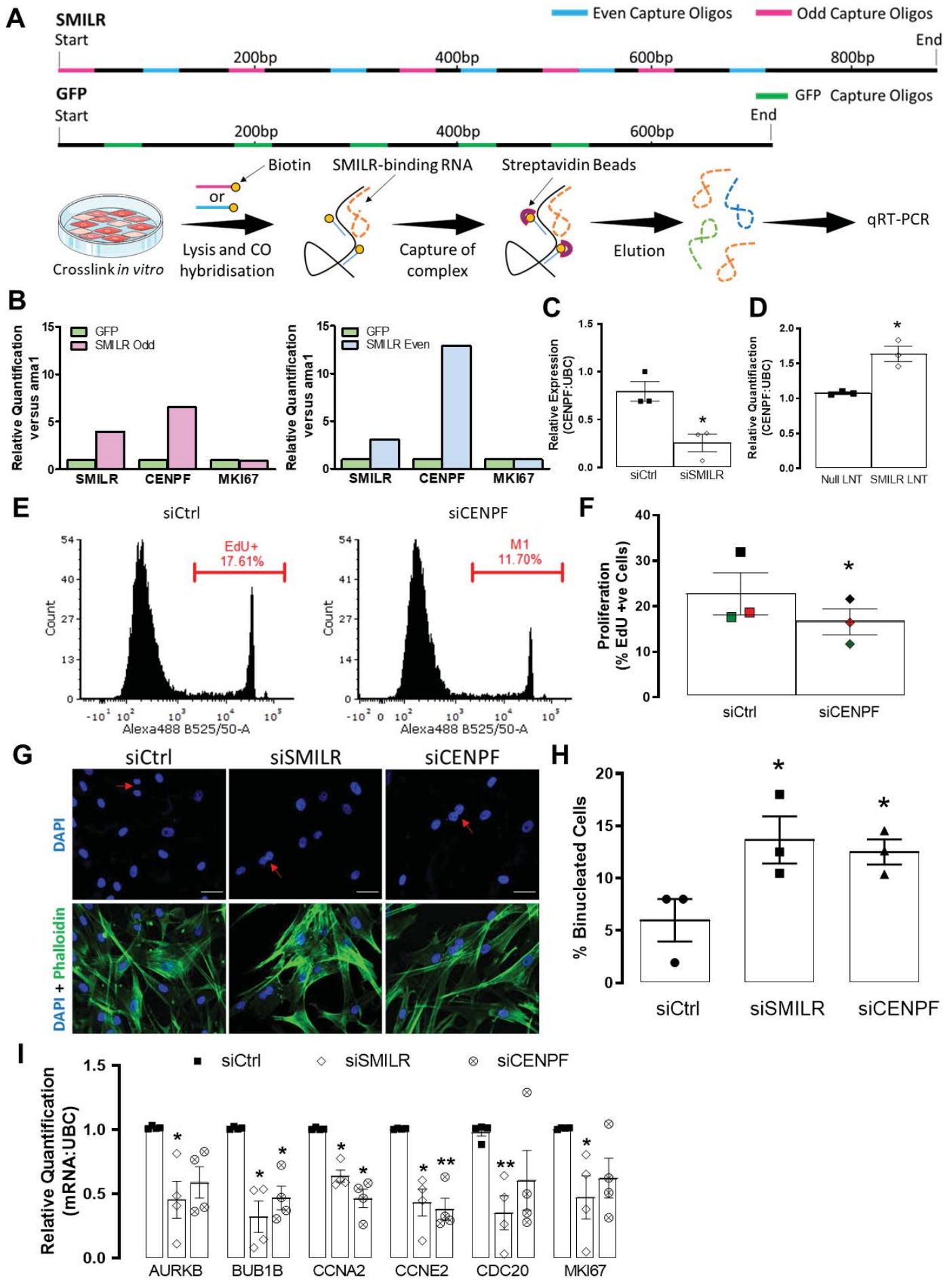

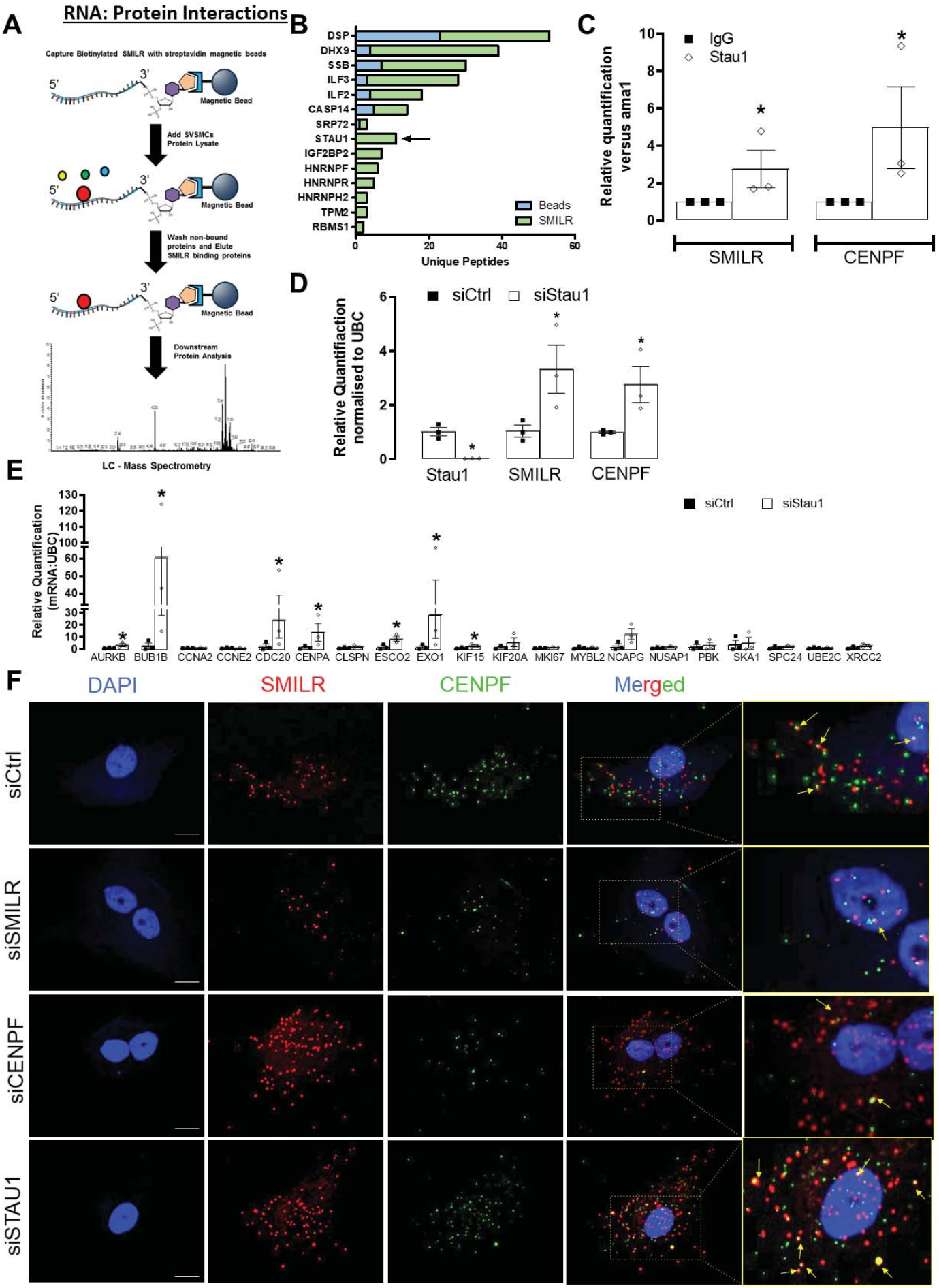

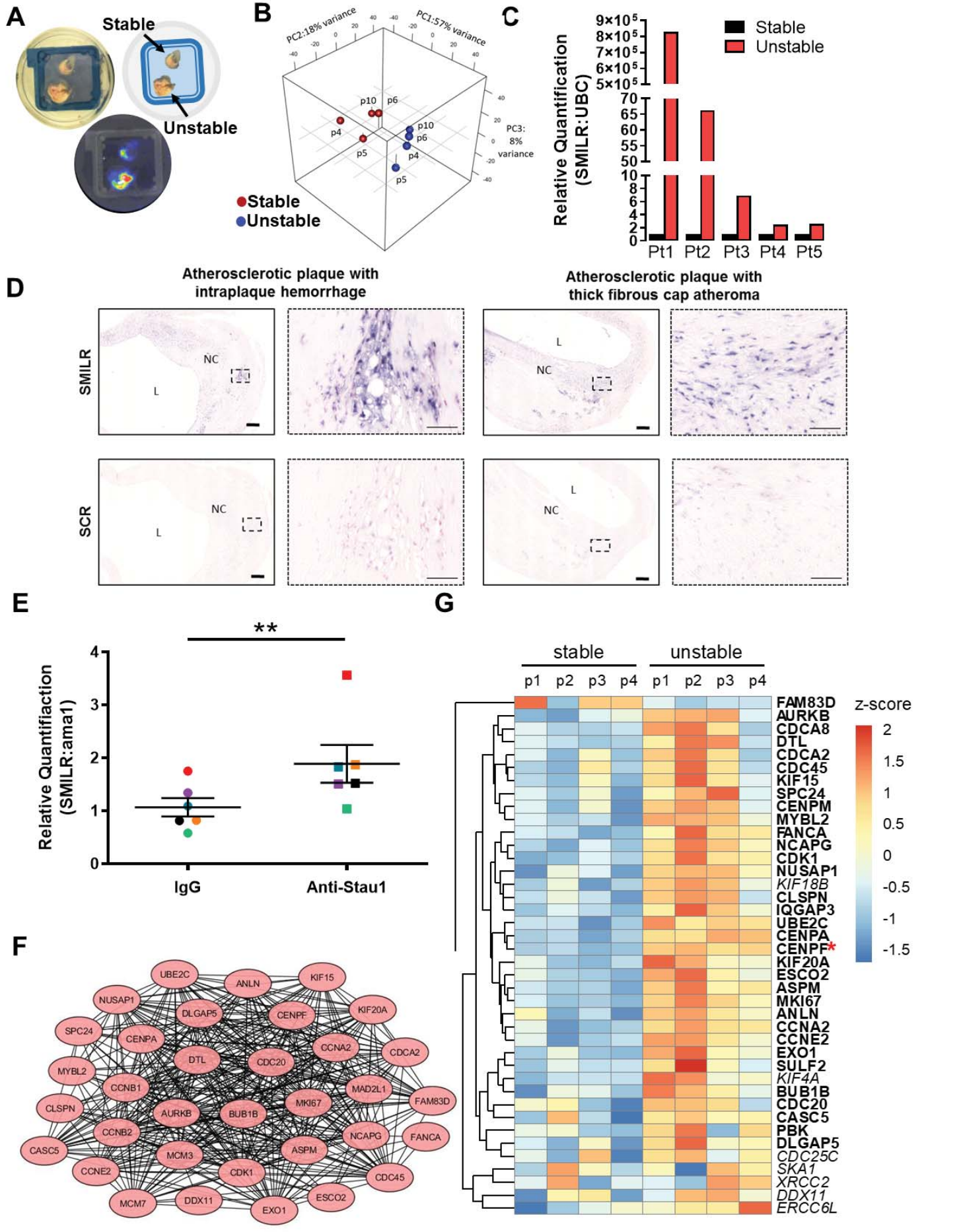

FIGURE 6